CHEMISTRY OF MATERIALS
Article

Chem. Mater. **2009,** *21,* 4905–4913 4905
DOI:10.1021/cm901987t

Optically pH and H_2O_2 Dual Responsive Composite Colloids through the Directed Assembly of Organic Dyes on Responsive Microgels

Weitai Wu, Ting Zhou, Michael Aiello, and Shuiqin Zhou*

Department of Chemistry and The Center for Engineered Polymeric Materials of College of Staten Island, and The Graduate Center, The City University of New York, 2800 Victory Boulevard, Staten Island, New York 10314

Received July 3, 2009. Revised Manuscript Received September 3, 2009

A novel type of smart composite materials based on the directed assembly of organic dyes on a responsive microgel template was prepared and investigated. We have chosen Calcon, a monoazo dye, as model organic dye molecules and the copolymer microgel of poly(N-isopropylacrylamide-acrylic acid-acrylamide) [p(NIPAM-AA-AAm)] as template with the pAA segments designed for inducing pH-sensitivity and the pAAm segments designed for directing the highly ordered assembly of dye molecules. Transmission electron microscopy, X-ray scattering, and light scattering were used to study the dye assembling structures and the pH-induced volume phase transitions of the composite microgels. The UV−vis absorption and photoluminescence properties of the composite microgels were respectively investigated at different pH values and H_2O_2 concentrations. The pH-induced shrinkage of the template microgels not only results in a systematic shift in the wavelength of bands, but also significantly increases the absorption and emission intensity. The composite microgels also exhibit a highly H_2O_2-sensitive fluorescence quenching. The pAAm-directed highly ordered assembling structure of dye molecules is critical to produce the unique pH/H_2O_2 dual responsive optical properties, which may find important applications in bioimaging and biosensing.

Introduction

Organic dye molecules offer many interesting properties for electronic and optical applications, and thus their assemblies possessing energy and charge transport properties have attracted considerable attention in materials as well as in biological sciences in the past decade.[1] Of particular interest is the formation of highly ordered and spectrally distinct dye assemblies produced through the interactions of dyes molecules with the host surface. Many different assembling host templates, such as SiO_2 and SnO_2 nanocrystallites,[2] zeolites,[3] gold nanoparticles,[4,5] polyoxometalate,[6] surfactants,[7] spermine,[8] helical peptide,[9] DNA,[10] polyelectrolytes,[11] dendrimers,[12,13] and block copolymer[14] have been applied to direct the assembly of organic dye molecules to form composite materials with well-organized structures and interesting optical properties. Azo dyes, the class of synthetic organic dyes containing the azo functionality, —N=N—, with attached aryl groups, are one example of a dye system whose assembly structure can change their optical properties. In addition, the optical properties of azo dyes are sensitive to hydrogen peroxide (H_2O_2), with the oxidation (decoloration) rate depending on the reaction environment.[15] H_2O_2 is an essential mediator in living systems; food, pharmaceutical, clinical, and industrial processes; environmental analysis; and many other fields. Thus, controlling the photophysical properties of fluorescent components by H_2O_2 may provide a new and versatile method to develop novel sensors. For example, ratiometric fluorescence detection of H_2O_2 has been developed on the basis of a dye platform to promote a change in its emission color upon reaction with H_2O_2.[16] The optical detection of glucose and acetylcholine esterase

*To whom correspondence should be addressed. E-mail: zhoush@mail.csi.cuny.edu. Tel:(718) 982-3897.

(1) (a) Hoeben, F. J. M.; Jonkheijm, P.; Meijer, E. W.; Schenning, A. P. H. J. *Chem. Rev.* **2005**, *105*, 1491. (b) *Supramolecular Dye Chemistry*; Wurthner, F., Ed.; Topics in Current Chemistry; Springer: Berlin, 2005; Vol. *258*.
(2) Nasr, C.; Liu, D.; Hotchandani, S.; Kamat, P. V. *J. Phys. Chem. B* **1996**, *100*, 11054.
(3) Ramamurthy, V.; Sanderson, D. R.; Eaton, D. F. *J. Am. Chem. Soc.* **1993**, *115*, 10438.
(4) Chandrasekharan, N.; Kamat, P. V.; Hu, J.; Jones, G.II *J. Phys. Chem. B* **2000**, *104*, 11103.
(5) Lim, I.-I. S.; Goroleski, F.; Mott, D.; Kariuki, N.; Ip, W.; Luo, J.; Zhong, C. J. *J. Phys. Chem. B* **2006**, *110*, 6673.
(6) Gao, S.; Cao, R.; Yang, C. *J. Colloid Interface Sci.* **2008**, *324*, 156.
(7) (a) Das, S.; Kamat, P. V. *J. Phys. Chem. B* **1999**, *103*, 209. (b) Guan, Y.; Antonietti, M.; Faul, C. F. J. *Langmuir* **2002**, *18*, 5939.
(8) Park, H. S.; Kang, S. W.; Tortora, L.; Nastishin, Y.; Finotello, D.; Kumar, S.; Lavrentovich, O. D. *J. Phys. Chem. B* **2008**, *112*, 16307.
(9) Cooper, T. M.; Stone, M. O. *Langmuir* **1998**, *14*, 6662.
(10) Hannah, K. C.; Armitage, B. A. *Acc. Chem. Res.* **2004**, *37*, 845.
(11) (a) He, J.-A.; Bian, S.; Li, L.; Kumar, J.; tripathy, S. K.; Samuelson, L. A. *J. Phys. Chem. B* **2000**, *104*, 10513. (b) Tao, X.; Li, J.; Mohwald, H. *Chem.—Eur. J.* **2004**, *10*, 3397.
(12) Karukstis, K. K.; Perelman, L. A.; Wong, W. K. *Langmuir* **2002**, *18*, 10363.
(13) (a) Grohn, F.; Klein, K.; Brand, S. *Chem.—Eur. J.* **2008**, *14*, 6866. (b) Willerich, I.; Ritter, H.; Grohn, F. *J. Phys. Chem. B* **2009**, *113*, 3339.
(14) Yu, H.; Qi, L. *Langmuir* **2009**, *25*, 6781–6786.
(15) Nango, M.; Iwasaki, T.; Takeuchi, Y.; Kurono, Y.; Tokuda, J.; Oura, R. *Langmuir* **1998**, *14*, 3272.
(16) Srikun, D.; Miller, E. W.; Domaille, D. W.; Chang, C. J. *J. Am. Chem. Soc.* **2008**, *130*, 4596.

Published on Web 09/22/2009

inhibitors by H_2O_2-sensitive CdSe/ZnS quantum dots has been reported.[17]

On the other hand, smart polymeric microgel templates, which can swell and shrink in response to external stimuli such as a change in temperature, pH, ionic strength, and light, have recently received great interest to host inorganic nanoparticles/nanorods assembled on their surface.[18−22] Such composites benefit from both the stimuli-responsive properties of polymers and the unique optical or magnetic properties of inorganic nanoparticles. For example, thermal responsive magnetic property[18] and photoluminescence property[19] have been observed when the γ-Fe_2O_3 and CdTe nanoparticles were respectively assembled on the surface of thermal sensitive poly(N-isopropylacrylamide) (pNIPAM) microgels, whereas pH tunable plasmon resonance of gold nanorods has been obtained when the gold nanorods were assembled on the surface of p(NIPAM-co-allylacetic acid) and p(NIPAM-co-acrylic acid-co-vinylimidazole) microgels.[20,22] Microgels offer several advantages over other polymer template systems: simple synthesis, easy functionalization, uniform size distribution, tunable dimension, potential biocompatibility, and a very short response time.[23] However, to the best of our knowledge, no study has been carried out to use the smart microgels serving as the template to direct and host organic dye molecular assembly.

In this work, we aim to develop a novel strategy to synthesize smart composite colloidal materials through the assembly of organic dye molecules onto a stimuli-responsive polymer microgel template in aqueous solution. The hybrid materials with fluorescent dye shell immobilized on smart polymer beads, combining the properties from both organic dye assembly and responsive polymers, can offer the possibilities for external switching and manipulation when applied to sensors and electronic/optical devices. We have chosen Calcon (see structure in Scheme 1), a monoazo dye, as model organic dye molecules to assemble onto the surface of smart copolymer microgels of poly(N-isopropylacrylamide-co-acrylic acid-co-acrylamide) [p(NIPAM-AA-AAm)]. The thermo-responsive pNIPAM component in the copolymer microgels is necessary to synthesize the nearly monodispersed microgel particles via the precipitation copolymerization because only the pNIPAM dominant p(NIPAM-AA-AAm) copolymer segments can have a lower critical solution temperature (LCST) and become insoluble to precipitate into the hydrophobic surfactant micellar core during the synthesis at a temperature above the LCST of the copolymer segments. While the fluorescent Calcon dye assemblies can act as an optical identification code and H_2O_2 sensitive component, the pH-sensitive poly(acrylic acid) (pAA) segments in the p(NIPAM-AA-AAm) microgels can induce the swelling and shrinking of the microgels, which can modify the physicochemical environment of the Calcon dye assemblies immobilized on their surface. As expected, the newly designed composite colloids have not only pH-responsive optical properties but also H_2O_2-sensitive photoluminescence (PL) for optical target identification. We found that the polyacrylamide (pAAm) segment in the microgels is important to direct the long-range ordered assembly of Calcon dye molecules on the microgel template. In contrast to the unstable free Calcon dye solution at neutral or basic pH values, the composite microgels from the Calcon assemblies immobilized on the microgel template possess very stable structure and optical properties in the whole investigated pH range of 2.74−8.92. The all-optical nanoscale pH/H_2O_2 "meter" reported here is likely to be highly useful in a wide range of applications within biology and biomedicine, where such a probe may prove to be a useful new tool for research, diagnosis, or monitoring.[17,24−29]

Scheme 1. Chemical Structure of Calcon Dye Molecule

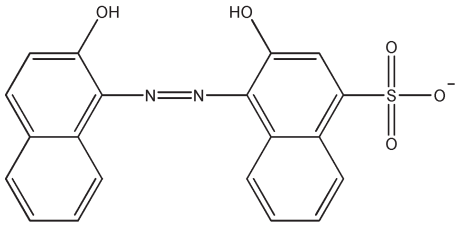

Experimental Section

Materials. Calcon dye molecule of 1-(2-Hydroxy-1-naphthylazo)-2-naphthol-4-sulfonic acid (Scheme 1) was purchased from

(17) Gill, R.; Bahshi, L.; Freeman, R.; Willner, I. *Angew. Chem., Int. Ed.* **2008**, *47*, 1676.
(18) Rubio-Retama, J.; Zafeiropoulos, N. E.; Serafinelli, C.; Rojas-Reyna, R.; Voit, B.; López-Cabarcos, E.; Eychmller, A.; Stamm, M. *Langmuir* **2007**, *23*, 10280.
(19) Agrawal, M.; Rubio-Retama, J.; Zafeiropoulos, N. E.; Gaponik, N.; Gupta, S.; Cimrova, V.; Lesnyak, V.; López-Cabarcos, E.; Tzavalas, S.; Rojas-Reyna, R.; Eychmller, A.; Stamm, M. *Langmuir* **2008**, *24*, 9820.
(20) (a) Karg, M.; Pastoriza-Santos, I.; Liz-Marzán, L.; Hellweg, T. *Chem. Phys. Chem.* **2006**, *7*, 2298. (b) Karg, M.; Lu, Y.; Carbo-Argibay, E.; Pastoriza-Santos, I.; Perez-Juste, J.; Liz-Marzán, L.; Hellweg, T. *Langmuir* **2009**, *25*, 3163.
(21) Kumar, V. P. R.; Samal, A. K.; Sreeprasad, T. S.; Pradeep, T. *Langmuir* **2007**, *23*, 8667.
(22) Das, M.; Mordoukhovski, L.; Kumacheva, E. *Adv. Mater.* **2008**, *20*, 2371.
(23) (a) Zhang, J.; Xu, S.; Kumacheva, E. *J. Am. Chem. Soc.* **2004**, *126*, 7908. (b) Zhang, J.; Xu, S.; Kumacheva, E. *Adv. Mater.* **2005**, *17*, 2336. (c) Das, M.; Sanson, N.; Kumacheva, E. *Chem. Mater.* **2008**, *20*, 7157. (d) Reese, C. E.; Mikhonin, A. V.; Kamenjicki, M.; Tikhonov, A.; Asher, S. A. *J. Am. Chem. Soc.* **2004**, *126*, 1493. (e) Zhang, Y.; Guan, Y.; Zhou, S. *Biomacromolecules* **2007**, *8*, 3842.
(24) Kim, S.; Pudavar, H. E.; Prasad, P. N. *Chem. Commun.* **2006**, *19*, 2071.
(25) Coakley, R. D.; Grubb, B. R.; Paradiso, A. M.; Gatzy, J. T.; Johnson, L. G.; Kreda, S. M.; O'Neal, W. K.; Boucher, R. C. *Proc. Natl. Acad. Sci. U. S. A.* **2003**, *100*, 16083.
(26) (a) Hirsch, L. R.; Stafford, R. J.; Bankson, J. A.; Sershen, S. R.; Rivera, B.; Price, R. E.; Hazle, J. D.; Halas, N. J.; West, J. L. *Proc. Natl. Acad. Sci. U.S.A.* **2003**, *100*, 13549. (b) Cognet, L.; Tardin, C.; Boyer, D.; Choquet, D.; Tamarat, P.; Lounis, B. *Proc. Natl. Acad. Sci. U.S.A.* **2003**, *100*, 11350.
(27) (a) El-Sayed, I. H.; Huang, X.; El-Sayed, M. A. *Nano Lett.* **2005**, *5*, 829. (b) El-Sayed, I. H.; Huang, X.; El-Sayed, M. A. *Cancer Lett.* **2006**, *239*(1), 129. (c) Lee, K. S.; El-Sayed, M. A. *J. Phys. Chem. B* **2006**, *110*, 19220.
(28) Hilderbrand, S. A.; Kelly, K. A.; Niedre, M.; Weissleder, R. *Bioconjugate Chem.* **2008**, *19*, 1635.
(29) (a) Polsky, R.; Gill, R.; Kaganovsky, L.; Willner, I. *Anal. Chem.* **2006**, *78*, 2268. (b) Niazov, T.; Shlyahovsky, B.; Willner, I. *J. Am. Chem. Soc.* **2007**, *129*, 6374.

Eastman-Kodak and all other chemicals were purchased from Aldrich. NIPAM was recrystallized from a hexane-toluene (a 1:1 volume ratio) mixture and dried in vacuum. AA was purified by distillation under reduced pressure to remove inhibitors. AAm, *N*,*N*′-Methylenebisacrylamide (MBAAm), ammonium persulfate (APS), sodium dodecyl sulfate (SDS, anionic), and Calcon dye sample were used as received without further purification. The water used in all experiments was of Millipore Milli-Q grade.

Synthesis of Template Microgels. The p(NIPAM-AA-AAm) microgels were prepared by free radical precipitation copolymerization of NIPAM, AAm, AA, and MBAAm using APS as an initiator. A mixture of NIPAM (1.405 g), AAm (0.080 g), AA (0.078 g), MBAAm (0.101 g), SDS (0.050 g), and water (95 mL) was poured into a 250 mL three-neck round-bottom flask equipped with a stirrer, a nitrogen gas inlet, and a condenser. The mixture was heated to 70 °C under a N_2 purge. After 30 min, 5 mL of 0.089 M APS was added to initiate the polymerization. The reaction was allowed to proceed for 5 h. The obtained p(NIPAM-AA-AAm) copolymer microgels were purified by centrifugation (Thermo Electron Co. SORVALL RC-6 PLUS superspeed centrifuge, 20000 rpm, 27 °C, 20 min), decantation, and then washed with water. The resultant microgel was further purified by 3 days of dialysis (Spectra/Por molecularporous membrane tubing, cutoff 12 000−14 000, the same below) against very frequently changed water at room temperature (∼ 22 °C). The same synthetic and purification procedure was used to synthesize the p(NIPAM-AAm) and p(NIPAM-AA) microgels, where the mixture of NIPAM (1.405 g)/AAm (0.160 g) and NIPAM (1.405 g)/AA (0.156 g) were respectively used as the comonomers for polymerizations.

Fabrication of p(NIPAM-AA-AAm)-Calcon Composite Colloids. Typically, 30 mL of p(NIPAM-AA-AAm) microgel suspension was stirred at room temperature for 30 min in a 100 mL round-bottom flask under a N_2 purge. At the same time, Calcon dye solution was prepared by dissolving 0.3478 g Calcon in 20 mL of water. After that, Calcon dye solution was added dropwise into the flask. The mixture was further stirred for 2 days. The resulting composite microgels assembled with Calcon dye molecules were then purified by at least 2 weeks dialysis against very frequently changed water at room temperature until the dialyzed water was transparent and colorless. In the whole process, the solution was kept in acidic condition of pH ∼4.8. Control experiments were also carried out by using p(NIPAM-AAm) microgel and p(NIPAM-AA) microgel, respectively, as templates to direct the assembly of Calcon dye molecules with the same approach under the same conditions.

Characterization. The FTIR spectra were recorded with a Nicolet Instrument Co. MAGNA-IR 750 Fourier transform infrared spectrometer. The microgel suspensions were dried on Spectra-Tech IR sampling cards with a PE substrate. The UV−vis absorption spectra were obtained on a Thermo Electron Co. Helios β UV−vis spectrometer. The PL spectra of the composite microgel dispersions at different pH values and different H_2O_2 concentrations were respectively obtained on a JOBIN YVON Co. FluoroMax-3 Spectrofluorometer. The pH values were measured on a METTLER TOLEDO SevenEasy pH meter. The transmission electron microscopy (TEM) images were taken on a FEI TECNAI transmission electron microscope at an accelerating voltage of 120 kV. Approximately 10 μL of the diluted composite microgel suspension was air-dried on a carbon-coated copper grid for the TEM measurements.

Small-angle X-ray scattering (SAXS) measurements were carried out on a Bruker NanoStar SAXS system. The microgel−dye composite colloidal dispersions as synthesized and purified in aqueous solution were directly placed into the capillary sample holders. The incident X-ray wavelength (λ) was tuned at 1.541 Å (Rotating Anode Cu-Ka source). A two-dimensional imaging plate was used in conjunction with an image scanner as the detection system. The sample to detector distance for SAXS was 72.5 mm. The scattering vector q is expressed as $q=(4\pi/\lambda)\sin(\theta/2)$, with θ being the scattering angle between the incident and the scattered X-rays. The d spacing of the ordered structures was calculated as $d=2\pi/q_{max}$.

Dynamic light scattering (DLS) was performed on a standard laser light scattering spectrometer (BI-200SM) equipped with a BI-9000 AT digital time correlator (Brookhaven Instruments, Inc.). A He−Ne laser (35 mW, 633 nm) was used as the light source. All colloidal dispersions were passed through Millipore Millex-HV filters with a pore size of 0.80 μm to remove dust before the DLS measurements. In DLS, the Laplace inversion of each measured intensity−intensity time correlated function can result in a characteristic line width distribution $G(\Gamma)$.[30] For a purely diffusive relaxation, Γ is related to the translational diffusion coefficient D by $(\Gamma/q^2)_{C\to 0,q\to 0}=D$, where $q=(4\pi n/\lambda)\sin(\theta/2)$, with n, λ, and θ being the solvent refractive index, the wavelength of the incident light in vacuo, and the scattering angle, respectively. $G(\Gamma)$ can be further converted to a hydrodynamic radius (R_h) distribution by using the Stokes−Einstein equation, $R_h=(k_BT/6\pi\eta)D^{-1}$, where T, k_B, and η are the absolute temperature, the Boltzmann constant, and the solvent viscosity, respectively.

Results and Discussion

Synthesis and Structure of p(NIPAM-AA-AAm)-Calcon Composite Microgels. Our strategy to prepare the optically pH/H_2O_2 dual responsive p(NIPAM-AA-AAm)−Calcon composite microgels involves the first synthesis of a pH-sensitive p(NIPAM-AA-AAm) microgel, followed by the assembly of H_2O_2-sensitive Calcon dye molecules on the microgel templates. The multiple-sensitive p(NIPAM-AA-AAm) microgels were synthesized from the free radical precipitation copolymerization of NIPAM, AAm (8.4 mol %), and AA (5.6 mol %) using MBAAm (4.3 mol %) as a cross-linker. The preparation of nearly monodispersed p(NIPAM-AA) microgels and p(NIPAM-AAm) microgels with well-controlled size and compositions has been well-established from the precipitation polymerization in water.[31] It has been reported that the contents of functional monomer AA or AAm in the pNIPAM-based microgels are nearly equal to their feeding compositions.[31c] On the other hand, a lower incorporation efficiency of AA into the p(NIPAM-AA) copolymer microgels was also reported, depending on the reaction condition and feeding amount of comonomers.[31d] In our present p(NIPAM-AA-AAm) microgels, the AA content of 5.4 mol % determined by titration is

(30) Chu, B. *Laser Light Scattering*, 2nd ed.; Academic Press: New York, 1991.

(31) (a) Zhou, S. Q.; Chu, B. *J. Phys. Chem. B* **1998**, *102*, 1364. (b) Ito, S.; Ogawa, K.; Suzuki, H.; Wang, B.; Yoshida, R.; Kokufuta, E. *Langmuir* **1999**, *15*, 4289. (c) Hoare, T.; Pelton, R. *Macromolecules* **2004**, *37*, 2544.Langmuir **2004**, *20*, 2123. (d) Kratz, K.; Hellweg, T.; Eimer, W. *Colloids Surf., A* **2000**, *170*, 137.

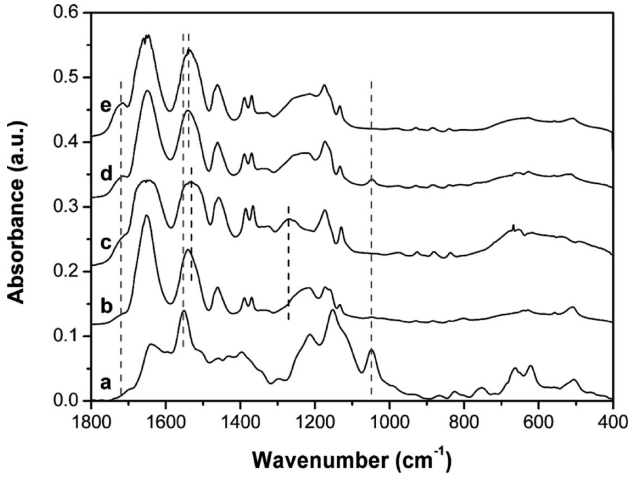

Figure 1. FTIR spectra of (a) free Calcon dye solution, (b) p(NIPAM-AA-AAm)−Calcon composite microgels, (c) template p(NIPAM-AA-AAm) microgels, (d) p(NIPAM-AA)−Calcon composite microgels, and (e) template p(NIPAM-AA) microgels.

very close to the feed composition. The reactivity ratio of AAm and AA had been narrowly defined with the Q and e values being $Q = 0.23$, $e = 0.54$ for the former, and $Q = 0.83$, $e = 0.88$ for the latter, respectively.[32] With the similar monomer reactivity, the resulted p(NIPAM-AA-AAm) copolymer microgels should have a randomly distributed functional AA and AAm group rich domains through the copolymer chains. The DLS characterization indicated that the obtained microgels are nearly monodispersed with a polydispersity index of $\mu_2/\langle\Gamma\rangle^2 = 0.001$ (see the Supporting Information).

Figure 1b shows the FTIR spectrum of the p(NIPAM-AA-AAm)-Calcon composite microgels. The FTIR spectra of free Calcon aqueous solution (7.0×10^{-3} g L^{-1}, approximately the same concentration as determined in the composite microgels) (Figure 1a) and p(NIPAM-AA-AAm) microgel template (Figure 1c) were also presented for comparison. In addition to the absorption maxima of amide I at 1649 cm^{-1} and amide II at 1533 cm^{-1}, a peak at 1712 cm^{-1} from the stretching of the uncharged dimerized or associated form of carboxylic acid group of AA units was observed in p(NIPAM-AA-AAm) microgels. After complexation with Calcon dye molecules, the p(NIPAM-AA-AAm)-Calcon composite microgels present a higher frequency amide II band at 1539 cm^{-1}, while nearly no change was observed in the absorption maxima of carboxylic acid groups in comparison with the microgel template. In addition, the strong signal at 1048 cm^{-1} observed in the free Calcon dye aqueous solution, which can be attributed to the symmetrical stretching vibration of the sulfonate groups,[11a] fainted nearly invisible in the p(NIPAM-AA-AAm)−Calcon composite microgels. On the basis of the change of the amide II and sulfonate bands, we deduce that the immobilization of Calcon assemblies on the p(NIPAM-AA-AAm) microgels is possibly via the reaction of the sulfonate group in Calcon dye molecules (in acid form) with the amino group in the

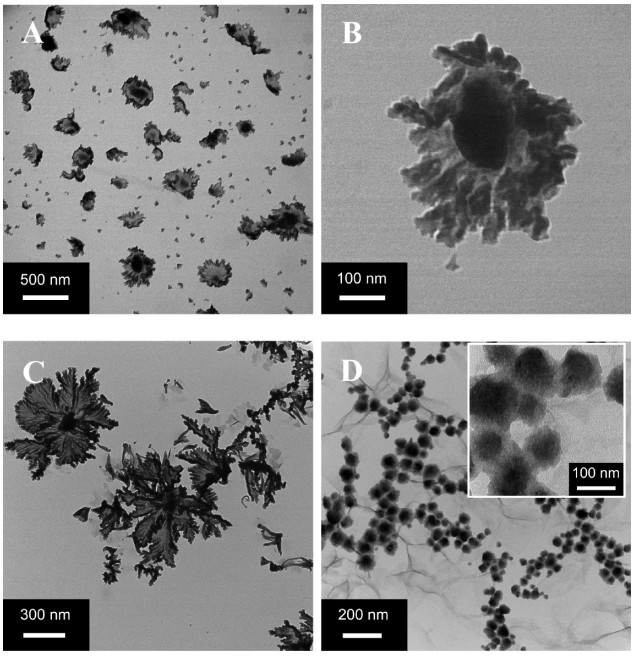

Figure 2. TEM images of the differently structured composite microgels of (A,B) p(NIPAM-AA-AAm)−Calcon, (C) p(NIPAM-AAm)−Calcon, and (D) p(NIPAM-AA)−Calcon, respectively.

pAAm segments of microgels.[33,34] To confirm this speculation, we did control experiments using p(NIPAM-AA) microgel as template to direct the assembly of Calcon dye molecules. The FTIR spectrum of p(NIPAM-AA)−Calcon composite microgels in Figure 1d indicate that the assemblies of the Calcon dye molecules on the p(NIPAM-AA) microgels almost have no effect on the characteristic absorption peaks of carboxylic acid, amide I and amide II groups in the p(NIPAM-AA) microgel template (Figure 1e) and the sulfonate groups in the free Calcon dye solution (Figure 1a). In such a design, the carboxylic acid groups in pAA segments can be mainly used to induce a pH-responsive volume phase transition of the microgels after the immobilization of Calcon dye assemblies stabilized by the amino groups of the pAAm segments.

Figure 2 shows typical TEM images of the composite microgels formed through the assembly of Calcon dye molecules on different microgel templates. Recognizing the importance of amino groups in the pAAm segments on the immobilization of Calcon assembly, we also investigated the composite microgels with p(NIPAM-AAm) microgel as template. Elegant core−shell structures were found on both the pAAm-containing composite microgels of p(NIPAM-AA-AAm)−-Calcon (A,B) and p(NIPAM-AAm)−Calcon (C). The dendritic shell of calcon assemblies (thickness 100−400 nm) represents a very wide variety of growth. It is possible that Calcon dye molecules were first bound to the microgel through the binding between the sulfonate groups in Calcon with the

(32) Broandrup, J.; Immergut, E. H.; Grulke, E. A. *Polymer Handbook*, 4th ed.; John Wiley & Sons: New York, 1999.

(33) (a) Kocjan, R.; wieboda, R.; Sowa, I. *Microchim. Acta* **2001**, *137*, 13. (b) Kocjan, R.; Blazewica, A.; Matosiuk, D. *Microchim. Acta* **2004**, *144*, 221.

(34) Wei, N.; Chen, J.; Zhang, J.; Wang, K.; Xu, X.; Lin, J.; Li, G.; Lin, X.; Chen, Y. *Talanta* **2009**, *78*(4−5), 1227.

amino groups in the microgels to form a well-oriented monomolecular layer of Calcon dye molecules. The hydrophobic well-oriented Calcon layer binds the subsequent layers of Calcon dye molecules through the hydrophobic interactions involving the π-electron rich structures.[33,35] The Calcon dye domains are "glued" by noncovalent $\pi-\pi$ interactions between Calcon dye molecules, which may be further stabilized by water species bridges.[36] Interestingly, a core−shell structure was also observed by using p(NIPAM-AA) microgels as semisoft template (D). However, the thickness of the Calcon dye shell reduced dramatically to about 50 nm or even thinner. In the absence of pAAm segments, the Calcon dye molecules might be first adsorbed randomly onto the surface of p(NIPAM-AA) microgels through a weaker hydrophobic interaction between the hydrocarbon chain domains of the microgels and the hydrophobic π-conjugated rings of Calcon dye molecules, which oriented the Calcon dye molecules laid on the surface of microgels with π-conjugated rings attaching on the hydrophobic sites. The flat orientation and weak attachment of the first Calcon molecular layer determines that the subsequent assembly of Calcon dye molecules through the noncovalent $\pi-\pi$ interactions cannot extend to long-range. The resulted p(NIPAM-AA)-Calcon composite microgels are also less stable with a trend to form aggregates in comparison with the p(NIPAM-AA-AAm)-Calcon composite microgels. It is clear that the pAAm segments in the microgel template have a strong influence on the assembly of Calcon dye molecules on the surface of microgel templates.

To differentiate the structures of the assembled Calcon dye shell on different microgel templates, SAXS measurements were carried out for the three composite microgels equilibrated in aqueous solutions. Figure 3 shows the SAXS patterns for the three composite microgels using p(NIPAM-AA-AAm) (a), p(NIPAM-AAm) (b), and p(NIPAM-AA) (c) microgels as semisoft templates, respectively. The SAXS curve from the free Calcon dye solution (Figure 3d) shows no signal within the tested q range. It should be mentioned that the scattering from the aqueous dispersion of template copolymer microgels is also very weak, and no any scattering peaks were observed in their SAXS curves. While the p(NIPAM-AAm)−Calcon composite microgels shows a sharp intensive peak at q = 0.13 Å^{-1}, the p(NIPAM-AA)−Calcon microgels shows a very broad weak peak with q_{max} = 0.34 Å^{-1}, which indicates that the Calcon dye molecules assembled to different structures on the p(NIPAM-AAm) and p(NIPAM-AA) microgel templates. The strong sharp peak observed at q_{max} = 0.13 Å^{-1} reveals that the Calcon dye molecules are assembled in a long-range highly ordered structure on

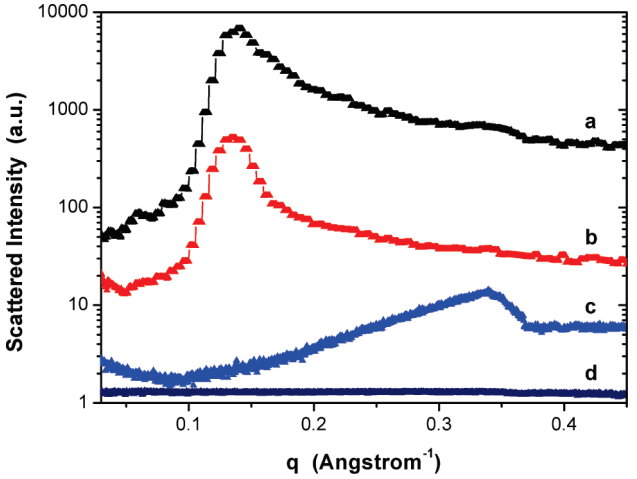

Figure 3. SAXS curves of the (a) p(NIPAM-AA-AAm)−Calcon, (b) p(NIPAM-AAm)−Calcon, and (c) p(NIPAM-AA)−Calcon composite microgel dispersions in aqueous solution formed on the different microgel templates. (d) SAXS curve of free Calcon dye solution.

the p(NIPAM-AAm) microgel template with an interdomain distance of 4.83 nm ($d=2\pi/q_{max}$).[37] The weak and very broad peak observed at q_{max} = 0.34 Å^{-1} indicates that the Calcon dye molecules are assembled in a short-range close packing of nonuniform Calcon domains on the p(NIPAM-AA) microgel template with an average interdomain distance of 1.85 nm. When the microgel template contains both the pAA and pAAm segments, the SAXS curve of the p(NIPAM-AA-AAm)−Calcon composite microgels shows a strong peak at q_{max} = 0.13 Å^{-1} observed in the p(NIPAM-AAm)−Calcon composite microgels and a very weak shoulder peak at q_{max} = 0.34 Å^{-1} observed in the p(NIPAM-AA)−Calcon composite microgels. These results indicated that the Calcon dye molecules are mainly assembled in a long-range highly ordered structure on p(NIPAM-AA-AAm) microgel template and a highly ordered packing of Calcon domains can only occur on pAAm-containing microgel templates, which are consistent with the TEM results. Our results demonstrated that the assembling structure of composite materials can be controlled by tailoring the functional groups on the template microgels to provide different interactions with the objected molecules, which can further affect the properties of the composite materials.

Volume Phase Transitions of p(NIPAM-AA-AAm)−Calcon Composite microgels. Figure 4 shows the pH-induced volume phase transition of the p(NIPAM-AA-AAm)−Calcon composite microgels in terms of the change of R_h measured at T = 22.1 °C and a scattering angle of θ = 45°. The pH of microgel dispersions was adjusted by using dilute HCl or NaOH aqueous solutions. Interestingly, after the immobilization of the thick shell of Calcon assemblies, the functional pAA segments on the copolymer chains of microgels can still result in a pH-responsive volume phase transition on the composite microgels. At pH below

(35) (a) Hu, J.; Guo, Y.; Liang, H.; Wan, L.; Jiang, L. *J. Am. Chem. Soc.* **2005**, *127*, 17090. (b) Rahman, G. M. A.; Guldi, D. M.; Campidelli, S.; Prato, M. *J. Mater. Chem.* **2006**, *16*, 62. (c) Ritchie, C.; Cooper, G. J. T.; Song, Y. F.; Streb, C.; Yin, H.; Parenty, A. D. C.; MacLaren, D. A.; Cronin, L. *Nat. Chem.* **2009**, *1*, 47. (d) Ma, Y.; Hao, R.; Shao, G.; Wang, Y. *J. Phys. Chem. A* **2009**, *113*, 5066.

(36) Lin, K.-J. *Angew. Chem., Int. Ed.* **1999**, *38*, 2730.

(37) Zhou, S. Q.; Xu, C.; Wang, J.; Gao, W.; Akhaverdiyeva, R.; Shah, V.; Gross, R. *Langmuir* **2004**, *20*, 7926.

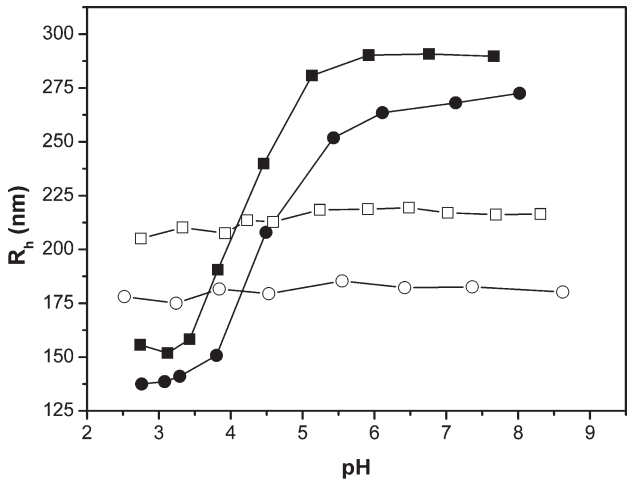

Figure 4. pH dependence of the average R_h value of the p(NIPAM-AA-AAm)−Calcon composite microgels (■), the p(NIPAM-AA-AAm) template microgels (●), the p(NIPAM-AAm)−Calcon composite microgels (□), and the p(NIPAM-AAm) template microgels (○), measured at 22.1 °C and a scattering angle $\theta = 45°$.

3.5, which is slightly lower than the pK_a value (~4.2) of the AA moiety,[38] the size of the composite microgels remained nearly a constant. When pH was above the pK_a of AA, the AA groups were gradually deprotonated. The Coulombic repulsion among the ionized carboxylate groups increased the osmotic pressure, resulting in the gradual increase in the size of composite microgels until all AA groups were deprotonated at pH > 5.1, where the microgels reached a maximum swelling ratio $[R_h(\text{charged})/R_h(\text{uncharged})]^3$ of 6.9. In comparison with the template p(NIPAM-AA-AAm) microgels, the size of the p(NIPAM-AA-AAm)−Calcon composite microgels is increased no matter if they are at the swollen or collapsed state because of the shell addition of Calcon assembly. Furthermore, the maximum swelling ratio of the p(NIPAM-AA-AAm)−Calcon composite microgels is only slightly higher than the swelling ratio $[R_h(\text{charged})/R_h(\text{uncharged})]^3 = 6.3$ of the template p(NIPAM-AA-AAm) microgels. These results implicated that the shell immobilization of the rigid Calcon assemblies has no significant effect on the swelling of the template core microgels, however, the pH increase may affect the interfacial environments between the microgel surface and the shell Calcon assemblies and the interactions of the Calcon domains in the assemblies, which can cause a slightly larger swelling ratio of the composite microgels over the template microgels.

pH-Sensitive UV−vis Absorption Properties of p(NIPAM-AA-AAm)−Calcon Composite Microgels. All aromatic compounds absorb electromagnetic energy but only those that absorb light with wavelengths in the visible range are colored.[39] Calcon (Scheme 1) contains two substituted aromatic rings, one with a hydroxyl substituent and the other with a hydroxyl and a sulfonate substituent, linked together by the azo (−N=N−) chromophores. Figure 5 shows the UV−vis spectra of the p(NIPAM-AA-AAm)−Calcon composite microgels (A) and the free Calcon dye solution (B), respectively, at different pH values. The free Calcon dye solution only shows a single peak with $\lambda_{max} = 511$ nm in the acidic pH range of 2.70−5.78. When the pH was increased to 7.08 and 9.13, the absorption λ_{max} shifted to 565 and 576 nm, respectively. In addition, the free Calcon dye solutions were unstable under neutral or basic pH values, and their color changed distinctly after setting for 1 day (Figure 5E). In contrast, the UV−vis absorption properties of the p(NIPAM-AA-AAm)−Calcon composite microgels show significant difference. First, the Calcon dye assemblies immobilized on the surface of the p(NIPAM-AA-AAm) microgels show two groups of absorption peaks. The band in the green wavelength region with $\lambda_{max} = 514-529$ nm at different pH values could be related to the assembled Calcon domains stowed by noncovalent $\pi-\pi$ interactions. Compared to the single band with $\lambda_{max} = 511$ nm from the free Calcon dye solution in the acidic pH range of 2.70−5.78, the band at $\lambda_{max} = 514-529$ nm has a red shift that indicates a J-aggregate in these assembled Calcon domains, while the new absorption band with $\lambda_{max} = 424-430$ nm at different pH values could be associated with the Calcon domains binding on the microgels, in which the delocalized electron systems somewhat shrink because of the electron-withdrawing substituents.[39] Second, the Calcon dye assemblies immobilized on the surface of the p(NIPAM-AA-AAm) microgels show a very similar absorption pattern in the whole investigated pH range of 2.74−8.92 covering all acidic, neutral, and basic conditions. These results indicate that the Calcon domains immobilized on the microgels have stable assembled structures even under the neutral and basic pH conditions, which can lead to stable optical properties. We found that the p(NIPAM-AA-AAm)−Calcon composite microgel dispersion is very stable with no detectable color change after setting for three months at room temperature (Figure 5D). Third, the decrease in pH value of the p(NIPAM-AA-AAm)−Calcon composite microgel dispersions from 8.92 to 2.74 could induce a systematic increase in absorption intensity and a blue shift of the λ_{max} for both the absorption bands from 430 to 424 nm, and from 529 to 514 nm, respectively. To confirm the reversibility of the pH-induced absorption change, we measured the UV−vis spectra of the composite microgel dispersions for three cycles with dialysis/pH adjustment. The absorption spectra were reproducible after the dialysis and pH adjustment, indicating that the pH-sensitive absorption property change is reversible. These optical property changes were unambiguously associated with the different swelling degrees of the template microgels followed by pH adjustment. The pH-induced gradual shrinking of the template microgels could bring the assembled Calcon domains closer and thus increase the interactions of Calcon domains, which further increases the absorption energy and intensity.

It should be mentioned that no systematic change in absorption intensity and wavelength was observed in the

(38) Cesarano, J.; Aksay, I. A.; Bleier, A. *J. Am. Ceram. Soc.* **1988**, *71*, 250.
(39) Pearce, C. I.; Lloyd, J. R.; Guthrie, J. T. *Dyes Pigm.* **2003**, *58*, 179.

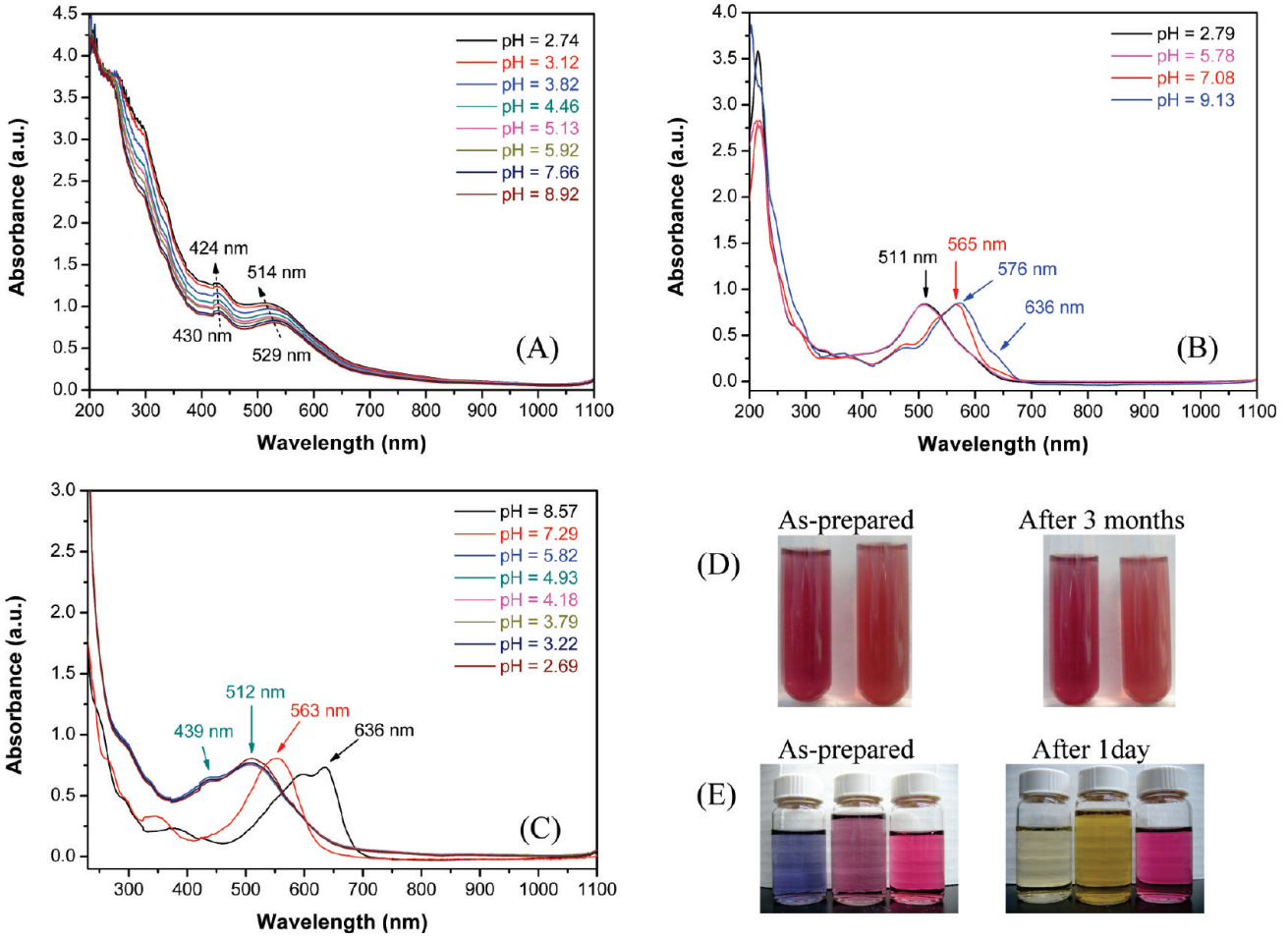

Figure 5. pH dependence of UV−vis absorption spectra of (A) the p(NIPAM-AA-AAm)−Calcon composite microgels, (B) the free Calcon dye solution (7.0×10^{-3} g L^{-1}), and (C) the p(NIPAM-AA)-Calcon composite microgels. The photographs present the color for (D) the p(NIPAM-AA-AAm)−Calcon composite microgels at pH 8.92 (left) and 2.74 (right), and (E) the free Calcon dye solutions at different pH values of 9.13 (left), 7.08 (middle), and 2.79 (right), respectively.

p(NIPAM-AA)-Calcon composite microgels in the pH range of 2.69−5.82 (Figure 5C) although the p(NIPAM-AA) template microgels are also pH-responsive. In comparison with the single band with $\lambda_{max} = 511$ nm from the free Calcon dye solution in a similar pH range of 2.70−5.78, the band at $\lambda_{max} = 512$ nm has nearly no change, while the band with $\lambda_{max} = 439$ nm again could be related to the Calcon domains that binds to the microgels. When the pH is increased to 7.29 and 8.57, the absorption λ_{max} shifted to 563 and 636 nm, respectively. All these results indicate that the optical properties of the Calcon assemblies attached on the p(NIPAM-AA) microgels is more close to those of free Calcon dye solution. It is clear that the pAAm-directed long-range highly ordered structure of Calcon assembly is critical to make the p(NIPAM-AA-AAm)−Calcon composite microgels possessing the pH-induced systematic optical property change.

pH-Sensitive PL Properties of p(NIPAM-AA-AAm)−Calcon Composite Microgels. The p(NIPAM-AA-AAm) microgels do not show PL in both swollen and collapsed states. However, this scenario changed when the Calcon assemblies were immobilized on the surface of the microgels. Figure 6 depicts the PL spectra of the p(NIPAM-AA-AAm)-Calcon composite microgels and the free calcon dye solutions (approximately the same concentration as determined in the composite microgels) measured at different pH values. Although only one broad weak emission peak was detected in the free Calcon dye solutions, two PL peaks in the visible wavelength range of 540−800 nm with greatly enhanced PL intensity were respectively observed in the p(NIPAM-AA-AAm)−Calcon composite microgels. The two different PL bands at the lower and higher wavelengths are possibly due to the two different types of Calcon domains discussed above (e.g., Calcon domains stowed by noncovalent $\pi-\pi$ interactions and Calcon domains binding on the microgels), or other unknown emission centers.[40] With the decrease in pH from 8.92 to 2.74, the PL peak at 613 nm is red-shifted to 622 nm and the emission band at 648 nm blue-shifted to 640 nm. In addition, the PL intensity of the p(NIPAM-AA-AAm)−Calcon composite microgel dispersions was dramatically enhanced with the gradual

(40) (a) Kagan, C. R.; Murray, C. B.; Bawendi, M. G. *Phys. Rev. B* **1996**, *54*, 8633. (b) Baldo, M. A.; O'Brien, D. F.; Thompson, M. E.; Forrest, S. R. *Phys. Rev. B* **1999**, *60*, 14422. (c) Liu, X. Y.; Bai, D. R.; Wang, S. *Angew. Chem., Int. Ed.* **2006**, *45*, 5475. (d) Swathi, R. S.; Sebastian, K. L. *J. Chem. Phys.* **2008**, *129*, 054703. (e) Okamoto, K.; Chithra, P.; Richards, G. J.; Hill, J. P.; Ariga, K. *Int. J. Mol. Sci.* **2009**, *10*, 1950.

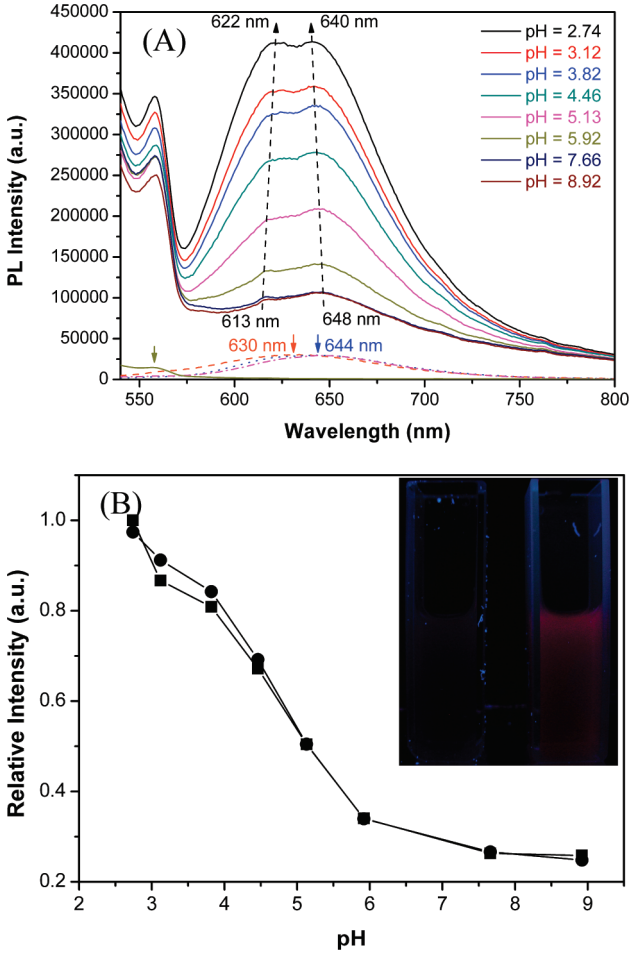

Figure 6. (A) pH-dependent PL spectra of the p(NIPAM-AA-AAm)−Calcon composite microgels obtained with the excitation wavelength at 520 nm. The PL spectra of Calcon dye solution (7.0×10^{-3} g L^{-1}) at different pH values of 2.79 (dash), 7.08 (dot), and 9.13 (dash dot), and p(NIPAM-AA-AAm) template microgels (solid line in the bottom) were also presented for comparison. (B) Relative PL intensity of the peak centered at 648 nm (■) and 613 nm (●) of the p(NIPAM-AA-AAm)−-Calcon composite microgels as a function of the pH of surrounding media. The photograph presents the color for the composite microgels dispersed at pH 8.92 (left) and 2.74 (right) under a 375 nm UV lamp.

shrinking of the template microgels, which could be distinguished easily by naked eye. However, the control experiments show that the pH has no effect on the PL intensity of the free Calcon dye solution. To visualize the relationship between the pH-induced volume phase transitions and the enhancement of the PL intensity of the p(NIPAM-AA-AAm)−Calcon composite microgels, we plotted the relative PL intensity as a function of pH (Figure 6B). The comparison of the pH-sensitive volume phase transition curve in Figure 4 with Figure 6B indicated that a conspicuous fluorescence increase occurred at nearly the same pH when the microgels began to shrink, clearly indicating the connection between the two phenomena. The change in delocalized electron systems should take the responsibility of the pH-sensitive PL property because the electron withdrawing or electron donating could weaken or intensify the PL of the chromophore by altering the overall energy of the delocalized electron system. However, the microgel directed Calcon assemblies could be significantly different from the free Calcon molecules.[41] It is proposed that the change in interactions among the neighboring Calcon domains at different swelling states of the microgels provides the second scenario for the change in delocalized electron systems. This can also cause a change of the local optical electric field around the Calcon domains.[42] The energy-transfer processes may also occur when the Calcon domains become close-packed.[41] Additionally, it could be related to the pH assisted population change of trap states near the valence band.[19,43] Nevertheless, it is clear that the p(NIPAM-AA-AAm) microgel directed Calcon dye assemblies in the close-packing states at lower pH values (e.g., pH $\leq$5.92) show significantly enhanced PL intensity in the visible wavelength range. The strong emission is particularly important for efficient in vivo optical imaging of biological system. The photos of the p(NIPAM-AA-AAm)−Calcon composite microgel dispersions at pH 8.92 and 2.74 under a 375 nm UV lamp demonstrated that the sample at pH 2.74 produced much brighter color.

H_2O_2−Sensitive PL Properties of p(NIPAM-AA-AAm)−-Calcon Composite Microgels. Figure 7A shows the time-dependent luminescence changes upon the reaction of p(NIPAM-AA-AAm)-Calcon composite microgels with H_2O_2 (0.4 mM) in a 0.005 M phosphate buffer of pH 5.03. The fluorescence of the composite microgels decreased rapidly with time, while only very mild decolorization of Calcon dye solution was observed in the absence of microgels or catalyst in the same time period, implying that H_2O_2 is indeed the component that induces the fluorescence quenching of the composite microgels. The hydrogenation of the azo $N=N$ bond in the presence of H_2O_2 presumably yields decolorization of azo dyes by splitting them into two amines.[39,44] Figure 7B shows the fluorescence quenching of the p(NIPAM-AA-AAm)-Calcon composite microgels upon interaction with H_2O_2 at different concentrations for a fixed time interval of 30 min. It can be seen that the composite microgels have much higher H_2O_2-sensitivity than the free Calcon dye solution in the investigated low H_2O_2 concentration range, verifying the advantage of p(NIPAM-AA-AAm)−Calcon composite microgels as a H_2O_2 sensor. It is known that numerous oxidases generate H_2O_2 as a product. For example, glucose oxidase (GOx) catalyzes the oxidation of β-D-glucose to produce D-glucono-δ-lactone and H_2O_2 over the pH range from 3.0 to 10.0 as the result of the unusual stability of this enzyme.[45] The newly designed optical H_2O_2 sensor of

(41) (a) Stoll, R. S.; Severin, N.; Rabe, J. P.; Hecht, S. *Adv. Mater.* **2006**, *18*, 1271. (b) Adachi, M.; Lockwood, D. J. *Self-Organized Nanoscale Materials*; Springer: New York, 2006.
(42) Kreibig, U.; Vollmer, M. *Optical Properties of Metal Clusters*; Springer, Berlin, 1995.
(43) (a) Kapitonov, A. M.; Stupak, A. P.; Gaponenko, S. V.; Petrov, E. P.; Rogach, A. L.; Eychmuller, A. *J. Phys. Chem. B* **1999**, *103*, 10109. (b) Walker, G. W.; Sundar, V. C.; Rudzinski, C. M.; Wun, A. W.; Bawendi, M. G.; Nocera, D. G. *Appl. Phys. Lett.* **2003**, *83*, 17.
(44) Cobley, C. M.; Campbell, D. J.; Xia, Y. N. *Adv. Mater.* **2008**, *20*, 748.
(45) Gibson, Q. H.; Swoboba, B. E. P.; Massey, V. *J. Biol. Chem.* **1964**, *239*, 3927.

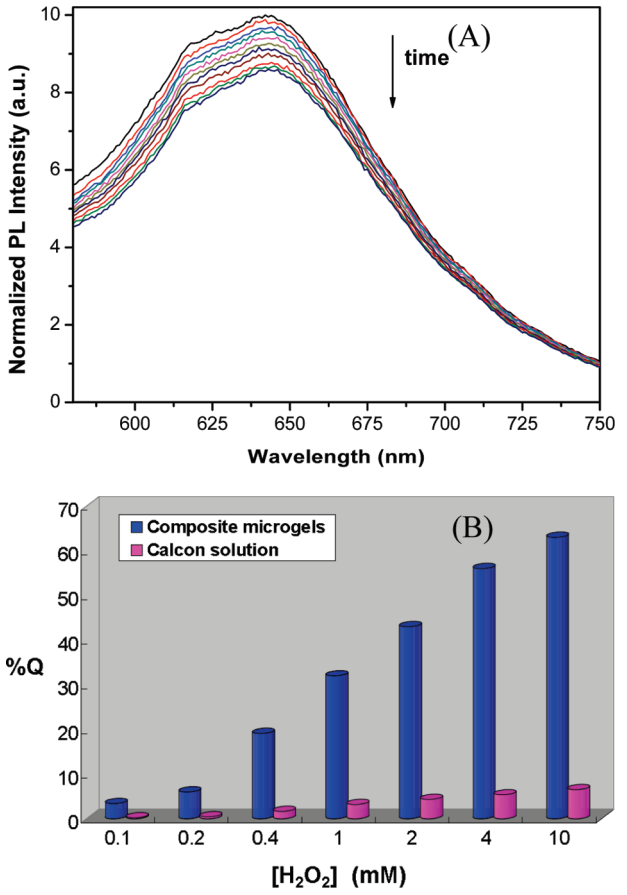

Figure 7. (A) Time-dependent fluorescence change of the p(NIPAM-AA-AAm)−Calcon composite microgels in the presence of 0.4 mM H_2O_2. Scans were taken at 3 min intervals from top to bottom except the bottom 3 curves (every 10 min). (B) Quenched fluorescence at 643 nm of the composite microgels upon interaction with different amount of H_2O_2 for a fixed time interval of 30 min. All measurements were performed in a 0.005 M PBS buffer solution at pH 5.03.

composite microgels may provide a simple and convenient way to determine glucose content directly with only microliter amount of serum samples.

Conclusion

The Calcon dye molecules can be directly assembled onto the semisoft pH-sensitive p(NIPAM-AA-AAm) microgel template. Both the covalent bonding between the amino groups of the pAAm segments in the microgels and the sulfonate groups in the dye molecules and the noncovalent $\pi-\pi$ interactions of conjugated rings in Calcon molecules are important to drive the formation and immobilization of the assembled Calcon layers. While the pAAm segments are critical to direct the Calcon molecules to form the long-range highly ordered assembling structures, the pAA segments can induce a pH-sensitive volume phase transition of the composite microgels. The resulting multifunctional p(NIPAM-AA-AAm)−Calcon composite microgels can be used for synchronous pH-sensitive imaging and optical sensing of H_2O_2 with a high sensitivity. The pH-induced shrinkage of the polymer networks could modify the delocalized electron systems of Calcon domains, resulting in a systematic shift of the absorption and emission bands and a gradual increase in absorption and great enhancement in PL intensity. The strong emission is particularly important for efficient in vivo optical imaging. The luminescence of the Calcon assemblies immobilized on the microgel template is also highly H_2O_2-sensitive. The increase in H_2O_2 concentration could significantly quench the PL of the composite microgels. In view of the uncommon photophysical properties of H_2O_2-sensitivity, we believe that it is promising to develop novel fluorescent probes for the chemical and biological sensors in the low concentration range based on the directed assembly of fluorescent organic dye molecules on the responsive microgels.

Acknowledgment. We gratefully acknowledge the financial support from the National Science Foundation for this project (CHE 0316078) and for the acquisition of X-ray scattering system (CHE 0723028). We also thank Dr. Yalin Wang at the imaging facility center of CUNY-CSI for his kind support on the TEM experiments.

Supporting Information Available: The typical hydrodynamic diameter distribution of the p(NIPAM-AA-AAm) template copolymer microgels determined from DLS (PDF). This material is available free of charge via the Internet at http://pubs.acs.org.